

Photoacoustic study of relaxation dynamics in multibubble systems in laser-superheated water

Sergey I. Kudryashov,* Kevin Lyon, and Susan D. Allen

Department of Chemistry and Physics, Arkansas State University, Jonesboro, Arkansas 72467-0419, USA

(Received 28 February 2006; published 4 May 2006)

Microsecond relaxation dynamics in a cavitating surface layer of bulk water superheated by a TEA CO₂ laser was studied using contact broadband photoacoustic spectroscopy. Damped nanosecond and microsecond oscillatory pressure-tension cycles recorded by an acoustic transducer are related to oscillations of steam bubbles of different sizes exhibiting strong dissipative losses and collective (coalescence and percolation) phenomena. These measurements also give important insight into basic parameters, characteristic spatial and temporal scales, and the mechanism of laser ablation of absorbing liquids in the thermal confinement regime.

DOI: [10.1103/PhysRevE.73.055301](https://doi.org/10.1103/PhysRevE.73.055301)

PACS number(s): 47.55.dd, 43.35.+d, 43.30.+m, 64.70.Fx

Bubble cavitation is an extremely random and not well-understood phenomenon that occurs in fluids in the form of bubble clouds, vortices, or filaments [1] and exhibits even in systems of two bubbles a number of interesting collective effects such as bubble attraction and repulsion, coalescence, and frequency up-conversion [2]. In such multibubble systems, bubbles, as quasi-steady-state density fluctuations, interact with each other via surrounding transient thermal and acoustic fields. In many cases such acoustic emission of oscillating bubbles provides the most efficient collective interaction (cross-talk) of neighboring bubbles, strongly affecting their dynamics [2,3] and, in particular, very interesting bubble collapse features such as acoustic (shock) wave emission [2,4] and sonoluminescence [5]. However, compared to systems of single or several visible bubbles, the collective dynamics of multiple bubbles in bulk cavitating fluids cannot be easily visualized by means of common high-speed or pump/probe optical techniques [2,4,6] or x-ray scattering technique [7], while in some cases such dynamics can be studied for bubbles on surfaces [8]. In contrast, acoustic emission of oscillating bubbles at different frequencies (typically in the MHz range) can be detected and spectrally resolved by means of broadband acoustic spectroscopic techniques, potentially providing important information about the characteristic frequencies of bubble oscillations, their relative abundance and lifetimes, as input thermodynamic parameters and characteristic temporal, and spatial scales for theoretical—phenomenological [9] or molecular dynamics [10,11]—simulations of explosive boiling phenomena. To our knowledge, there have been no such acoustic studies of collective bubble dynamics and interbubble interactions in multibubble systems to date.

In this paper we report use of a contact broadband photoacoustic (PA) spectroscopy to study microsecond relaxation dynamics of multiple micron-sized steam bubbles synchronously generated in a micron-thick layer on a free surface of bulk water superheated above its explosive boiling threshold by a TEA CO₂ laser. In this geometry, acoustic waves emitted by bubbles interact with other bubbles during

their propagation within the surface layer providing inter-bubble interaction. The acoustic waves exhibit strong damping of their rarefaction phases due to enhanced absorption of tensile waves in bubbly liquids [10,12] driving bubble growth (ultrasonic cavitation). Because the superheated layer is thin, these waves can escape it without a significant interaction with bubbles in the perpendicular (normal) direction to the layer. The corresponding oscillatory pressure-tension acoustic transients $p(t)$ recorded normal to the layer in the acoustic farfield using a state-of-art broadband point acoustic transducer carry rich information about these bubbles and their interactions. The recorded transients, when subjected to Fourier analysis, give characteristic bubble oscillation frequencies and amplitudes of such oscillation modes (i.e., relative abundances of bubbles of different sizes), while widths of corresponding spectral lines represent bubble lifetimes. These important basic parameters of bubbles measured using broadband PA spectroscopy, may provide unique information about the dynamics of individual bubbles and their collective interactions.

In the PA experiments a 10.6 μm , TEA CO₂ laser beam (TEM₀₀, 100 mJ/pulse, the 100 ns (FWHM) initial spike storing about $\gamma_1 \approx 50\%$ of the total energy, with a 0.7 μs tail, 1 Hz repetition rate) was focused by a ZnSe spherical lens (focal distance $L=10$ cm, Gaussian focal spot radius $\sigma_{1/e} \approx 0.2$ mm) at normal incidence onto the free surface of bulk deionized water in a container made of a plastic tube of a height $H \approx 8$ mm. Laser energy was varied using a number of clear polyethylene plastic sheets (20% attenuation per piece) and was measured in each pulse by splitting off a part of the beam to a pyroelectric detector with digital readout (Gentec ED-500). The front quartz window (thickness $h \approx 3$ mm) of a fast acoustic transducer (LiNbO₃ piezoelement, nearly flat response in the 1–100 MHz frequency range, manufactured in the Laboratory of Laser Optoacoustics at Moscow State University) served as the bottom of the container. The relatively small laser spot on the water surface provided PA measurements in the acoustic farfield, resulting in differential shapes of recorded transients [13] distorted by diffraction (the diffraction parameter $(H+h)/L_D \sim 1$, where $L_D = \pi f \times \sigma_{1/e}^2 / C_l$ is the diffraction length [13] for acoustic pulses with frequencies $f=1-10^2$ MHz and the speed of sound in water $C_l \approx 1.4$ km/s [14]). A LeCroy storage oscil-

*Electronic address: skudryashov@astate.edu,
sergeikudryashov@yahoo.com

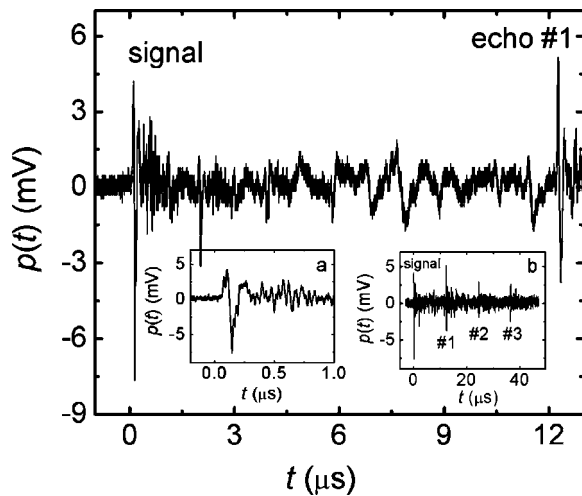


FIG. 1. Acoustic waveform $p(t)$ recorded in water at $F \approx 3.5 \text{ J/cm}^2$. The insets show the same waveform on the time scales $t = -0.1 - 1.5 \mu\text{s}$ (a) and $t = -3 - 47 \mu\text{s}$ (b) with the $8\text{-}\mu\text{s}$ delay subtracted. The main bipolar signal and acoustic echoes are marked as “signal” and #1–3.

loscope (Wavepro 940) was used to record electrical voltage transients (Fig. 1) (delayed by the $8 \mu\text{s}$ needed for the corresponding acoustic transients to propagate in water and the quartz window) from the transducer, while no transients were detected without the laser pulse heating the water surface or with the transducer not in contact with the water container.

PA measurements were performed at various laser fluences F in the range $0.8 - 11 \text{ J/cm}^2$ (Fig. 2), where the near-spinodal explosive boiling of a superheated near-surface water layer of a thickness equal to a temperature-dependent absorption depth for the CO_2 -laser radiation, $\delta_w(10.6 \mu\text{m}) \approx 8 - 10 \mu\text{m}$ [15], accompanied by visible expulsion of a water jet occurs above the corresponding threshold $F_B \approx 1.7 \pm 0.3 \text{ J/cm}^2$ (see similar thresholds for similar TEA CO_2 -laser temporal pulse shapes in Refs. [16,17]). At $F \approx F_B$ the volume energy density in the superheated water layer at the end of the laser spike, $\varepsilon \approx \gamma_1 \times F_B / \delta_w^*$ ($10.6 \mu\text{m}$) $\approx 1.0 \text{ kJ/cm}^3$ [for $\gamma_1 \approx 0.5$ and

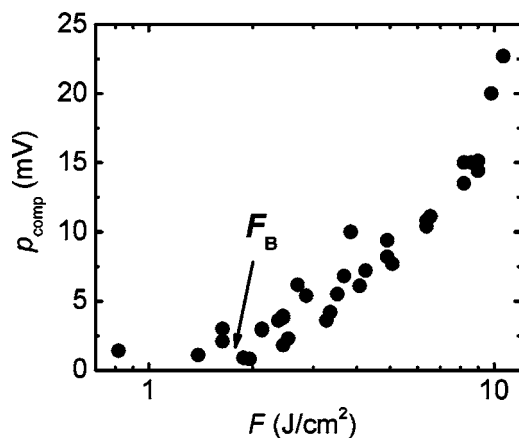


FIG. 2. Compressive pressure p_{comp} as a function of laser fluence F . $F_B \approx 1.7 \text{ J/cm}^2$ is the corresponding explosive boiling threshold of water.

$\delta_w^*(10.6 \mu\text{m}) \approx 9 \mu\text{m}$ [15]], corresponds to maximum water temperatures $T = 590 - 600 \text{ K}$ [18] which are close to spinodal temperatures of water at positive external pressures P , $T_{\text{spin}}(P > 0) \approx (0.9 - 1)T_{\text{crit}} \approx 580 - 647 \text{ K}$ [18]. For $F \geq F_B$, the main bipolar acoustic pulse ($t = 0 - 0.2 \mu\text{s}$, inset (a) in Fig. 1) with the FWHM parameter equal to that of the laser spike exhibits threshold-like increase of the compressive pressure amplitude p_{comp} (Fig. 2), indicating the appearance of the explosive boiling effect [19]. Its actual temporal shape with a predominant compression (positive) phase transforms to a bipolar one with predominant rarefaction (negative) phase due to the diffraction effect in the acoustic farfield [13] where data acquisition was performed.

Accompanying the intense bipolar pulse at $F \geq F_B$ is a pronounced oscillatory tail that begins right after the laser spike ($t > 0.2 \mu\text{s}$) and lasts for $t = 0 - 12 \mu\text{s}$ (Fig. 1), where the signal is not perturbed by the acoustic echoes in the water layer appearing after time instants $t \approx 12, 24, \text{ and } 36 \mu\text{s}$, respectively (inset (b) in Fig. 1). This tail represents cavitation dynamics of steam bubbles in the form of pressure-tension cycles—bubble growth [$p(t) > 0$], shrinkage and collapse [$p(t) < 0$], and rebound [the next positive stage of $p(t)$] [1,2]—at characteristic frequencies $f \approx 20 - 40 \text{ MHz}$ (Fig. 1). Similar oscillations (typical $f = 16, 20, \text{ or } 25 - 30 \text{ MHz}$ [16,17,20]) were earlier detected in water at similar laser fluences, if point acoustic detectors were used to avoid the destructive interference of acoustic waves emitted by multiple bubbles at different positions in the near-surface laser-superheated water layer, and were interpreted as oscillations of bubbles produced around micron-sized solid dust (e.g., soot) species suspended in water [16]. However, in this work no oscillations were observed on a μs time scale in the acoustic transients at $F < F_B$, indicating that the origin of such multi-MHz bubbles is related to sub- μs explosive homogeneous boiling in the near-surface superheated water layer at $F \geq F_B$.

Temporal evolution of bubble clouds in explosively boiling water is clearly observable in the time frame $t = 0 - 12 \mu\text{s}$ (Fig. 1), where low-amplitude pressure oscillations occur at different frequencies f decreasing as a function of time: $f \approx 15 - 40 \text{ MHz}$ at $t = 0.2 - 1.4 \mu\text{s}$, $f \approx 5 - 15 \text{ MHz}$ at $t = 1.5 - 3 \mu\text{s}$, while for $t > 3 \mu\text{s}$ there are very pronounced 1 and 2 MHz oscillations. This dynamics of various frequency components is more evident in amplitude FFT spectra of the waveform (Fig. 3) taken in the interval $t = 0 - 12 \mu\text{s}$ using a $1 \mu\text{s}$ time window. These spectra show rapid population of the lower-frequency (1–5 MHz) oscillation modes at the expense of the higher-frequency (20–40 MHz) modes. However, when plotted versus time (Figs. 4(a) and 4(b)), the amplitudes $p(f)$ of all these modes demonstrate a damping effect during $t = 2 - 4 \mu\text{s}$ with lifetimes $\tau(f)$ about $1 \mu\text{s}$ [$\tau(f)$ values extracted from half-widths of corresponding spectral modes in Fig. 3 are $0.7 - 0.9 \mu\text{s}$], which is consistent with complete permanent decrease of the total acoustic power $\Pi(t) \sim |p(t)|^2$ for $t \leq 1.5 - 2 \mu\text{s}$ (see the inset in Fig. 4). Importantly, at the end of this process the amplitude $p(1 \text{ MHz})$ of the characteristic oscillation at the lowest frequency $f \approx 1 \text{ MHz}$ (Fig. 3) exhibits a gradual increase until $t \approx 8 \mu\text{s}$ (Fig. 4), when the final population decay of the

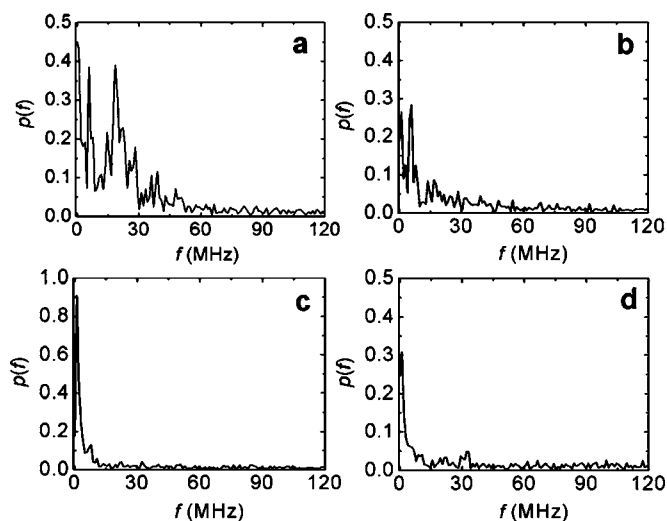


FIG. 3. Amplitude FFT spectra $p(f)$ of the acoustic waveform in Fig. 1 taken using a $1 \mu\text{s}$ time window in the time intervals $t=0.3\text{--}1.3 \mu\text{s}$ (a), $3.3\text{--}4.3 \mu\text{s}$ (b), $7.3\text{--}8.3 \mu\text{s}$ (c), and $9.3\text{--}10.3 \mu\text{s}$ (d).

mode occurs at a rate 0.7 MHz [$\tau(1 \text{ MHz}) \approx 1.5 \mu\text{s}$]. Other modes with intermediate frequencies $f \approx 18.4$ and 5.9 MHz show in Fig. 4 similar, but smaller peaks at earlier $t \approx 3$ and $4 \mu\text{s}$, respectively. Surprisingly, these experimental results including characteristic dynamics of vapor bubbles in *bulk* water, their oscillation frequencies and damping times are in good agreement with similar results for *surface* microbubbles in liquid nitrogen [8].

The microsecond damping of steam bubble oscillations and the consequent “red” shift of their amplitude FFT spectra accompanied by the final damping of bubble oscillations at the lowest frequency of 1 MHz can be interpreted in terms of separate physical processes experimentally demonstrated for individual or twin bubbles [2] and illustrated in MD simulations [10]. In particular, one can consider, respectively: (1) dissipative losses to acoustic emission, heat diffusion, and viscous effects during $t \leq 3 \mu\text{s}$ for *all* initial steam bubbles (oscillation frequencies of $1\text{--}40 \text{ MHz}$) nucleated via homogeneous boiling mechanism at temperatures $T \approx 590\text{--}600 \text{ K}$ and pressures $P^* \sim 10^7 \text{ Pa}$ (the saturated vapor pressure of water $P_w^s(593 \text{ K}) \approx 10^7 \text{ Pa}$ [18]) during the 100 ns laser spike; (2) the resulting reduction of size and energy of these bubbles leading to their enhanced coalescence (in the collapse phase [2]) during $t \approx 3\text{--}8 \mu\text{s}$ and giving larger bubbles oscillating more slowly (the “red” spectral shift); (3) coalescence and coarsening of the intermediate bubbles for $t \leq 8 \mu\text{s}$ to the maximum possible size (diameter) $D_{\text{max}} \leq \delta_w^*(10.6 \mu\text{m}) \approx 9 \mu\text{m}$ followed during $t \approx 8\text{--}11 \mu\text{s}$ by collapse of the final bubbles resulting in expulsion of

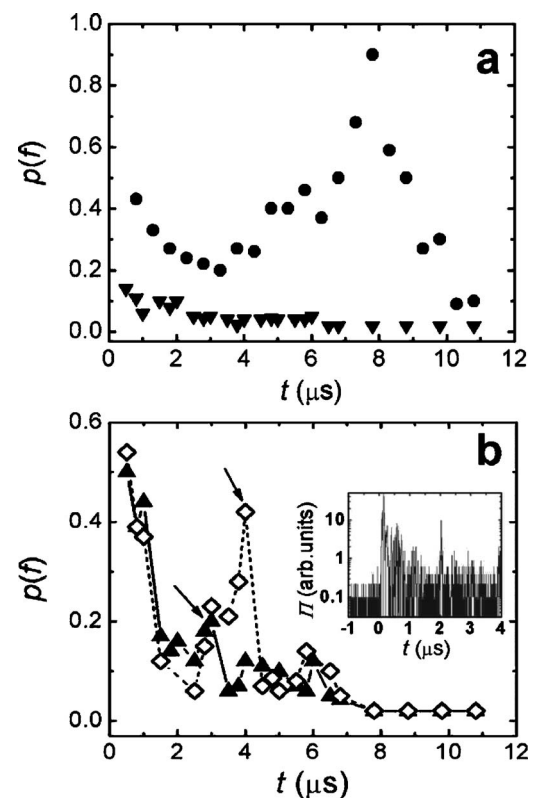


FIG. 4. Time dependences of FFT amplitudes $p(f)$ for main spectral modes in Figs. 1 and 3: (a)— 1 MHz (circles), 28.4 MHz (squares), and 36.5 MHz (down triangles); (b)— 5.9 MHz (rhombs) and 18.6 MHz (up triangles); the arrows show positions of their intermediate peaks. The inset demonstrates relaxation of the acoustic power Π during the time interval $t=0\text{--}1.5 \mu\text{s}$.

microjets (micron-sized water droplets) [12,16,21] or by further growth of the bubbles that is confined within the superheated cavitating water layer (percolation) and may ended up with spallation of the partially disintegrated top liquid layer [10].

In conclusion, in these photoacoustic spectroscopic studies of a thin cavitating layer on a surface of bulk water superheated by TEA CO_2 laser radiation up to its liquid/vapor spinode curve, we have revealed firm indications of microsecond dynamics of steam bubbles including their relaxation, cavitation, coarsening, and percolation resulting in the final removal (lift-off) of the disintegrated liquid layer in the form of vapor/droplet mixture. Providing the first direct experimental support for the qualitative results of corresponding molecular dynamics simulations, our results may give also important insights into basic thermodynamic parameters, temporal, and spatial scales, as well as the mechanism of laser ablation in the thermal confinement regime.

- [1] D. H. Trevena, *Cavitation and Tension in Liquids* (Adam Hilger, Bristol, 1987).
- [2] P. Testud-Gioanneschi, A. P. Alloncle, and D. Dufresne, *J. Appl. Phys.* **67**, 3560 (1990).
- [3] R. I. Nigmatulin, I. Sh. Akhatov, N. K. Vakhitova, and E. Sh. Nasibullaeva, in *Non-linear Acoustics at the Turn of Millennium: ISNA 15* (AIP, New York, 2000), ISBN 1-56396-945-9, CP524.
- [4] W. Hentschel and W. Lauterborn, *Appl. Sci. Res.* **38**, 225 (1982).
- [5] O. Baghdassarian, H.-C. Chu, B. Tabbert, and G. A. Williams, *Phys. Rev. Lett.* **86**, 4934 (2001); M. P. Brenner, S. Hilgenfeldt, and D. Lohse, *Rev. Mod. Phys.* **74**, 425 (2002); D. J. Flannigan and K. S. Suslick, *Nature* **434**, 52 (2005).
- [6] E. A. Brujan, G. S. Keen, A. Vogel, and J. R. Blake, *Phys. Fluids* **14**, 85 (2002).
- [7] V. Kotaidis and A. Plech, *Appl. Phys. Lett.* **87**, 213102 (2005).
- [8] K. F. MacDonald, V. A. Fedotov, S. Pochon, B. F. Soares, N. I. Zheludev, C. Guignard, A. Mihaescu, and P. Besnard, *Phys. Rev. E* **68**, 027301 (2003).
- [9] I. Hansson, V. Kedrinskii, and K. A. Mørch, *J. Phys. D* **15**, 1725 (1982).
- [10] E. Leveugle and L. V. Zhigilei, *Appl. Phys. A: Mater. Sci. Process.* **A79**, 753 (2004); E. Leveugle, D. S. Ivanov, and L. V. Zhigilei, *ibid.* **A79**, 1643 (2004).
- [11] S. Amoruso, R. Bruzzese, M. Vitiello, N. N. Nedialkov, and P. A. Atanasov, *J. Appl. Phys.* **98**, 044907 (2005).
- [12] G. Paltauf and H. Schmidt-Kloiber, *Appl. Phys. A: Mater. Sci. Process.* **A62**, 303 (1995).
- [13] V. E. Gusev and A. A. Karabutov, *Laser Optoacoustics* (AIP, Melville NY, 1993).
- [14] I. S. Grigor'ev and E. Z. Meilikhov, *Fizicheskie Velichini* (Energoatomizdat, Moscow, 1991) (in Russian).
- [15] R. K. Shori, A. A. Walston, O. M. Stafsudd, D. Fried, and J. T. Walsh, Jr., *IEEE J. Sel. Top. Quantum Electron.* **7**, 959 (2001).
- [16] A. F. Vitshas, L. M. Dorozhkin, V. S. Doroshenko, V. V. Korneev, L. P. Menakhin, and A. P. Terentiev, *Sov. Phys. Acoust.* **34**, 43 (1988).
- [17] F. V. Bunkin, A. A. Kolomensky, V. G. Mikhailevich, S. M. Nikiforov, and A. M. Rodin, *Sov. Phys. Acoust.* **32**, 21 (1986), and references therein.
- [18] V. P. Skripov, E. N. Sinitsyn, P. A. Pavlov, G. V. Ermakov, G. N. Muratov, N. V. Bulanov, and V. G. Baidakov, *Thermophysical Properties of Liquids in the Metastable State* (Gordon and Breach, New York, 1988).
- [19] S. I. Kudryashov, Ph.D. thesis, Moscow State University, 1999.
- [20] D. C. Emmony, T. Geerken, and H. Klein-Baltnik, *J. Acoust. Soc. Am.* **73**, 220 (1983).
- [21] K. Hatanaka, M. Kawao, Y. Tsuboi, H. Fukumura, and H. Masuhara, *J. Appl. Phys.* **82**, 5799 (1997); D. Kim and C. P. Grigoropoulos, *Appl. Surf. Sci.* **127-129**, 53 (1998); I. Apitz and A. Vogel, *Proc. SPIE* **4961**, 48 (2003).